ISSN: 2447-3359

REVISTA DE GEOCIÊNCIAS DO NORDESTE

Northeast Geosciences Journal

v. 11, nº 1 (2025)

https://doi.org/10.21680/2447-3359.2025v11n1ID30834

Geochemical characterization in the hypersaline floodplain influenced by upstream estuarine system in the Apodi-Mossoró River

Caracterização geoquímica das áreas hipersalinas sob influência do alto curso estuarino do Rio Apodi-Mossoró

Carlos Daniel Silva e Souza[1]; Raquel Franco de Souza[2]; Diógenes Félix da Silva Costa[3]

[1] Federal University of Rio Grande do Norte (UFRN), Regional Graduate Program in Development and Environment (PRODEMA), Natal/RN, Brazil. Email: daniel.souza.cd@gmail.com
ORCID: https://orcid.org/0000-0002-5310-7341

[2] Federal University of Rio Grande do Norte (UFRN), Department of Geology/CCET, Natal/RN, Brazil. Email: raquel.franco@ufrn.com.br
ORCID: https://orcid.org/0000-0001-8818-0605

[3] Federal University of Rio Grande do Norte (UFRN), Department of Geography/CCHLA & Câmara Cascudo Museum, Natal/RN, Brazil. Email: diogenes.costa@ufrn.com.br
ORCID: https://orcid.org/0000-0002-4210-7805

Abstract: The fluvial-marine plains are environments closely related to continental and oceanic factors, since they are located in coastal zones and form high salinity soils. In the northern area of Rio Grande do Norte (RN), due to the geomorphological and climatic conditions, these plains are characterized as hypersaline environments. The fluvial-marine floodplain of the Apodi-Mossoró River is located in the estuarine zone, with flattened areas and impermeable soils that favor the damming of river and marine waters. In this research, the geochemical conditions of the soil were investigated in the upper estuarine system located in the Brazilian semiarid region; for this, soil samples were collected with different depths in different hypersaline environments. The laboratory analyzes indicated a soil with high concentrations of Na^+, Ca^{2+} and Mg^{2+}, presenting sodic classification, salic character and moderately alkaline condition; these characteristics reflect the influence of the semiarid climate and progressive evaporation of sea water in the supratidal area, favoring the precipitation of salts in the upper estuarine course. The granulometry of the sediments, in turn, indicated the predominance of finer particles such as silt and clay in the textural composition of the soil.

Keywords: Wet areas; Salinity; Estuarine environment.

Resumo: As planícies flúvio-marinhas são ambientes de estrita relação com os fatores continentais e oceânicos, uma vez que estão localizadas em zonas costeiras e formam solos de alta salinidade. Na área setentrional do Rio Grande do Norte (RN), em razão das condições geomorfológicas e climáticas, estas planícies são caracterizadas como ambientes hipersalinos. A planície de inundação flúvio-marinha do rio Apodi-Mossoró localiza-se na zona estuarina, possuindo áreas planas e solos impermeáveis que favorecem o represamento das águas fluviais e marinhas. Nessa pesquisa, foram investigadas as condições geoquímicas do solo no alto curso estuarino localizado no semiárido brasileiro; para isso, foram coletadas amostras de solo com profundidades diferenciadas em ambientes hipersalinos distintos. As análises laboratoriais indicaram um solo com grandes concentrações de Na^+, Ca^{2+} e Mg^{2+}, apresentando classificação sódica, caráter sálico e condição moderadamente alcalina; essas características são reflexos da influência do clima semiárido e evaporação progressiva da água do mar na área de supramaré, favorecendo a precipitação de sais no alto curso estuarino. A granulometria dos sedimentos, por sua vez, indicou predominância de partículas mais finas como silte e argila na composição textural do solo.

Palavras-chave: Áreas úmidas; Salinidade; Ambiente Estuarino.

Received: 17/11/2022; Accepted: 12/12/2023; Published: 14/05/2025.

1. Introduction

The hypersaline condition, in general terms, is the result of the relationship between geomorphological and climatic aspects (FANG; LIU; KEARNEY, 2005; PANKOVA et al., 2018) that act, predominantly, in tropical areas of the globe where potential evapotranspiration rates often exceed pluviometric precipitation (COSTA et al., 2014a; RIDD; STIEGLITZ, 2002; FREIRE et al., 2021; PEDROTTI et al., 2015) and, consequently, influence the physical and chemical conditions of the soils.

Thus, hypersalinization occurs when salinity exceeds 50 g/L^{-1} (KJERFVE et al., 1996) and causes the first salts to precipitate on the surface (OREN, 2009; COSTA et al., 2015). This specific characteristic can affect different types of environments, such as: fluvial-marine floodplains (ALBUQUERQUE et al., 2014a; ALBUQUERQUE et al., 2014b; COSTA et al., 2014a), lagoons (GORDON, 1999; KJERFVE et al., 1996), swamps/marshes (SHEN et al., 2018; BORNMAN; ADAMS, 2009; GANJU et al., 2017), deserts (HERRERO; WINDORF; CASTANEDA, 2015), marine plains with evaporitic formations (LAST, 1989; MEES; SINGER, 2006; BROWN, 2021) and, in certain instances, they develop through the impoundment of water bodies influenced by the sea (PINHEIRO; MORAIS, 2010).

In hypersaline fluvial-marine plains, the deposition of sediments is directly influenced by negative estuaries (MIRANDA; CASTRO; KJERFVE, 2002), an interface for the contact, mixing, and dilution of marine and fluvial waters (TUNDISI; TUNDISI, 2008); this process, coupled with the flat topography and poor drainage (JESUS; BORGES, 2020), allows the low-energy astronomical tide water to advance into the supratidal zone, facilitating physical, chemical, and biological processes (SUGUIO, 2003; GUEDES; SANTOS; CESTARO, 2016).

Therefore, geochemistry in marine-influenced systems follows the sequence pattern based on the differentiated solubility and precipitation of the elements present in seawater, dominated by Na^{+} and Cl^{-} ions and smaller quantities of SO_4^{-2}, Mg^{+2}, Ca^{+2}, K^{+1}, CO_3^{-2} and HCO_3^{-1} (SILVA; SCHREIBER; SANTOS, 2000). In arid and semi-arid regions, minerals such as gypsum, halite, iron hydroxide and alkaline salts precipitated in the topsoil may crystallize (FANG; LIU; KEARNEY, 2005; GRIGORE; TOMA, 2017), a condition that directly interferes with the development of vegetation. (UCHOA; HADLICH; CELINO, 2008; JESUS; BORGES, 2020).

Considering the growing occupation of hypersaline environments, it is essential to obtain information to better understand the dynamics of these ecosystems (HERRERO; WINDORF; CASTANEDA, 2015), especially through a pedological approach. The characterization and classification of the soils present in these systems is substantial to support the issue of conservation and sustainability in threatened areas (ALBUQUERQUE et al., 2014a). Owing to this challenge, environments affected by salts have been the subject of research in several countries, mainly Australia, Bulgaria, France, Greece, India, Italy, Israel, Mexico, Puerto Rico, Slovenia and Spain (OREN, 2009).

In Brazil, the largest fluvial-marine hypersaline plains are located mainly in the state of Rio Grande do Norte, between the estuarine zones of the Apodi-Mossoró, Piranhas-Açu and Galinhos-Guamaré rivers, which have had economic potential since the colonial period, when crystallized salt was already used for human and animal consumption (COSTA et al., 2013); currently, the solar saltworks in the region produce around 95% of all the salt consumed in the country (ROCHA, 2005; COSTA et al., 2022).

In the Apodi-Mossoró River floodplain, the area is mainly occupied by salt and shrimp farming activities (SILVA; COSTA, 2022); however, despite the significant overall development of the plain, the upper estuarine course is characterized as the least anthropized zone. Based on the hypothesis that the geomorphological accumulation landforms of the upper estuarine course exhibit soils with distinct characteristics, this study aims to assess and characterize the geochemical conditions of the soils in these environments.

2. Methodology

2.1 Study area

The study area under investigation is situated in the coastal zone of the northern coastline of the state of Rio Grande do Norte, between the municipalities of Areia Branca, Grossos and Mossoró (Figure 1). The spatial delimitation of the research pertains to the upper estuarine reach of the Apodi-Mossoró River floodplain.

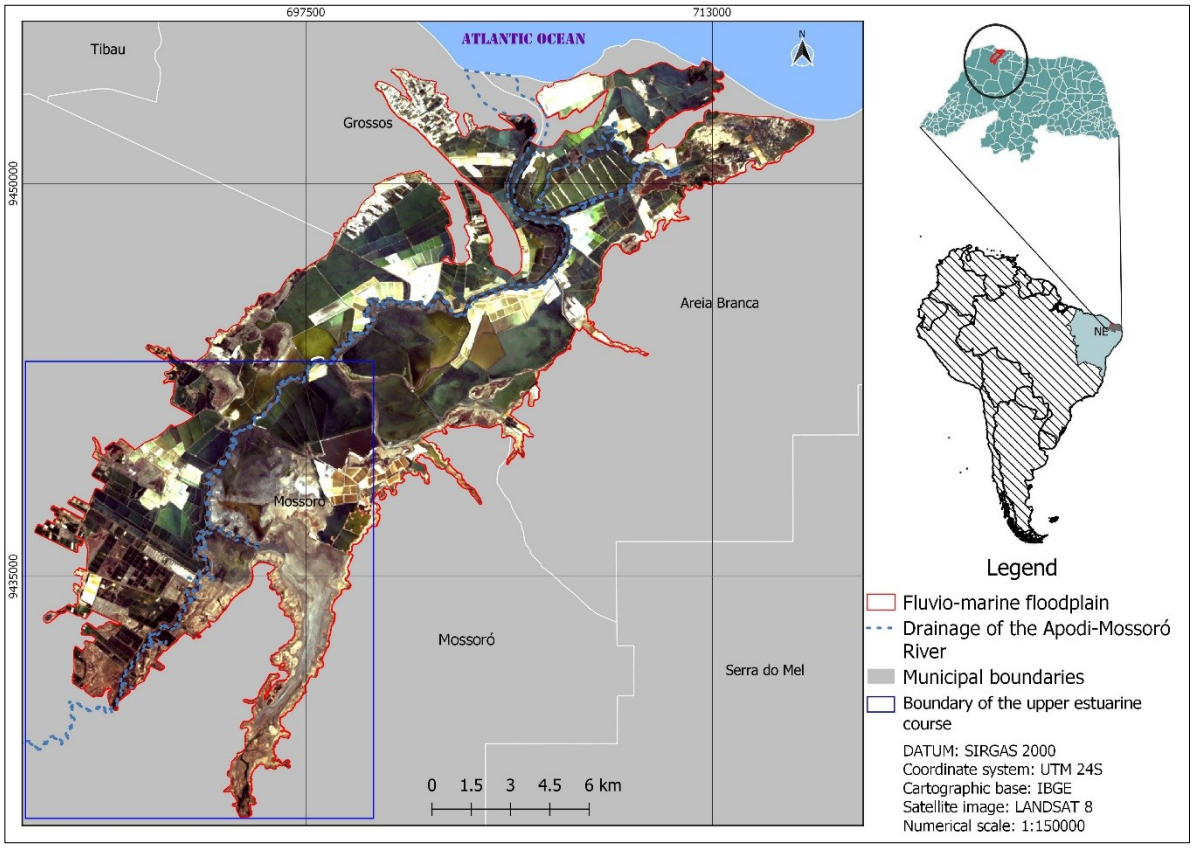

Figure 1 – Location map of the Apodi-Mossoró River estuarine floodplain.
Source: Authors (2022).

In the second half of the year, the flow of fresh water from the river decreases considerably, favoring the permanence of salt water in the estuarine region, which favors the hypersalinization of the estuary (COSTA; ROCHA; CESTARO, 2014), directly influencing local pedogenesis, through the concentration of evaporites from sediment precipitation; furthermore, its specific conditions foster to the development of the region (COSTA et al., 2014a; COSTA et al., 2022).

Under these conditions, the surrounding vegetation has an endemic floristic structure, consisting of shrub and herbaceous formations, perfectly adapted to the semiarid climate, characterized as 'savanna-like' Caatinga vegetation with a predominance of deciduous spiny plants (IBGE, 2012).

In areas near the estuary, where the salinity level is critical, halophytic mangrove vegetation predominates, consisting of four species: *Avicennia germinans*, *Avicennia schaueriana*, *Laguncularia racemosa*, and *Rhizophora mangle*; saline fields of salinas and apicuns correspond to sun-exposed areas with sandy soil and sparse shrub vegetation. (COSTA; ROCHA; CESTARO, 2014; GUEDES; SANTOS; CESTARO, 2016; COSTA; SOUZA; SOUZA, 2021).

2.2 Methodological Procedures

Soil collection involved three sample sets with spatially distributed points in distinct hypersaline wetland areas, located in the upper estuarine course zone of the fluvio-marine floodplain of the Apodi-Mossoró River (Table 1): the fluvial plain (Apf), the fluvio-lagoonal plain (Apflg), and the fluvio-marine plain (Apfm); the terminology is consistent with the geomorphological accumulation models proposed by Silva and Costa (2022) for the study area (Figure 2). The points and their respective depths were organized as follows: in the Apf, the points were P-234 (05-15cm), P-235 (20-30cm), P-236 (10-20cm), P-237 (10-20cm), and P-238 (20-30cm); in the Apflg, P-239 (05-15cm), P-240 (05-15cm), and P-241 (05-15cm); and in the Apfm, P-317 (0-15cm), P-318 (0-15cm), P-319 (0-15cm), and P-320 (0-15cm) (Figure 3).

Table 1 – Characterization of the sampling points in the fluvio-marine floodplain of the Apodi-Mossoró River.

Sample	UTM coordinates	Elevation	Accumulation models	Vegetation	Environmental characterization
P-234	694.925mE 9.427.686mN	3m	Fluvial plain	Halophytic herb	Saline field; bank of the Carmo River (a tributary of the Apodi-Mossoró River) with the presence of Algaroba (*Prosopis juliflora*) and Carnaúba (*Copernicia prunifera*); terrace surrounded by Caatinga.
P-235 P-236	695.211mE 9.428.213mN	4m	Fluvial plain	Halophytic herb	Saline field near the bank of the Carmo River, with a predominance of Algaroba (*P. juliflora*).
P-237 P-238	696.052mE 9.429.896mN	4m	Fluvial plain	Absence	Desertic terrace with sparse halophytic vegetation in higher-elevation areas within the flood zone.
P-239	696.849mE 9.434.776mN	4m	Fluvial-lagoonal plain	Absence	Section with high eolian dynamics, with silt and clay during the dry season; absence of herbaceous and halophytic vegetation. Soil subject to deflation.
P-240	695.832mE 9.435.931mN	1m	Fluvial-lagoonal plain	Absence	Connection between the Apodi-Mossoró River and the Carmo River, in front of the saltworks; flooded area without herbaceous vegetation.
P-241	695.444mE 9.435.197mN	1m	Fluvial-lagoonal plain	Absence	Hypersaline plain zone frequently flooded by the tide.
P-317	690.575mE 9.431.481mN	3m	Fluvio-marine plain	Halophytic herb	Saline field with sparse herbaceous vegetation and the presence of shrub vegetation nearby; area located close to shrimp farming ponds.
P-318	690.412mE 9.431.434mN	3m	Fluvio-marine plain	Mangrove	Gamboa with a small mangrove grove (*Avicennia germinans*); area located near shrimp farming ponds.
P-319	694.600mE 9.440.462mN	2m	Fluvio-marine plain	Mangrove	Environment located between the estuary and solar saltworks, predominantly covered by mangrove.
P-320	690.363mE 9.461.098mN	2m	Fluvio-marine plain	Absence	Saline field showing soil saturation and absence of vegetation; herbaceous and shrub vegetation were observed in the surrounding area.

Source: Authors (2022).

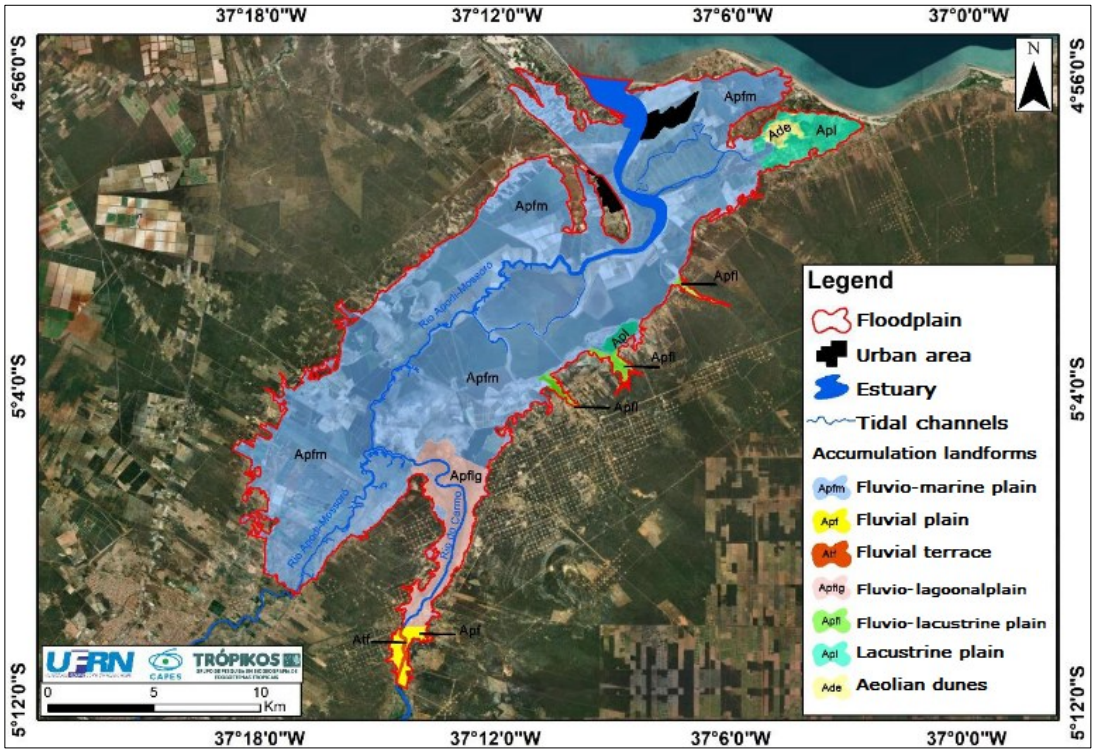

Figure 2 – Accumulation landforms in the lower course of the Apodi-Mossoró River. Source: Silva and Costa (2022).

The samples consisted of extracting approximately 2 kg of soil using a helical auger. In areas where the soil exhibited saturation, a gardening shovel was used. After collection, the soil samples were quartered into smaller quantities, around 1.0 kg, to be sent to the analysis laboratory (LASAP-UFERSA) for the determination of macronutrient values (Ca^{2+}, Mg^{2+}, Na^{+}, K^{+}, and P), potential acidity, granulometry, organic matter (OM) content, cation exchange capacity (CEC), base sum and saturation, exchangeable aluminum saturation, electrical conductivity (EC), exchangeable Sodium Percentage (ESP), and hydrogen ion concentration (pH).

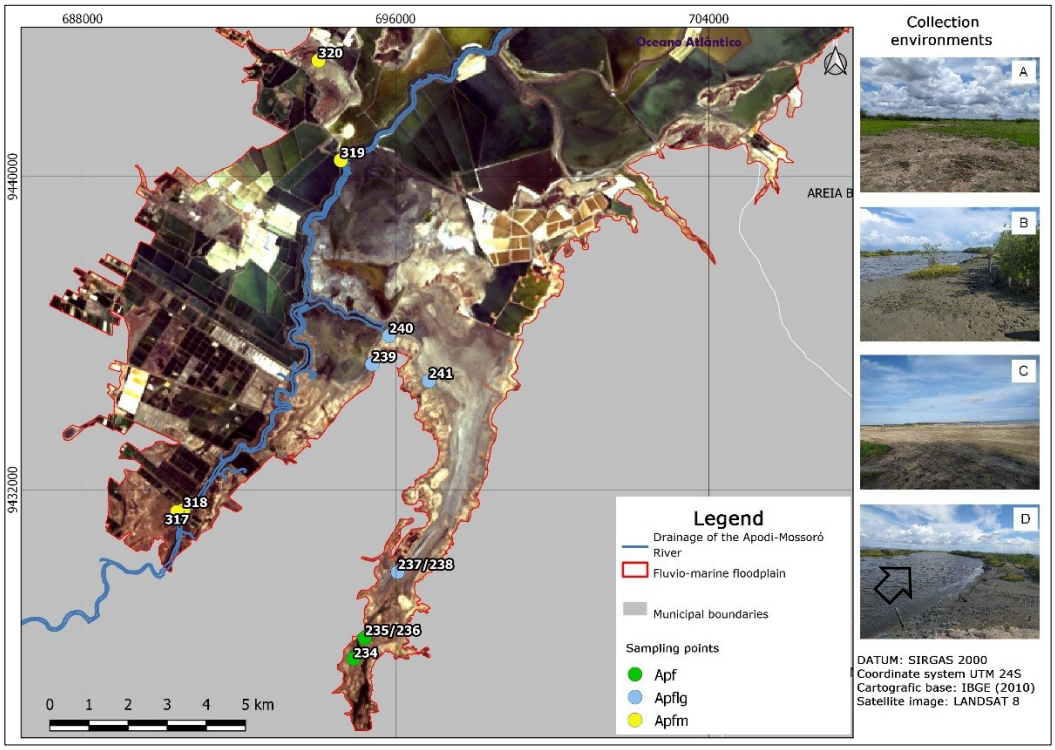

Figure 3 – Map of the spatial distribution of sampling points in the upper estuarine course of the fluvio-marine floodplain of the Apodi-Mossoró River. The photos to the right of the map are located in the Fluvio-Marine Plain (Apfm). A: Environment with halophytic herbaceous vegetation (light green in the center of the photo); B: Mangrove forest (on the right); C: Saline field/apicum (with little or no vegetation); D: Estuary (arrow indicates tidal advance). Source: Authors (2022).

2.3 Laboratory Methods

In the laboratory, the samples were identified and stored in an oven at 60°C for drying. Thereafter, the soil was crushed, sieved, and divided into smaller portions for chemical and physical analyses. The laboratory procedures were based on Embrapa's *Manual of Soil Analysis Methods* (2017).

The physical analyses determined the grain size distribution of the sediment samples by quantifying sand, silt, and clay. For this purpose, the pipette method was used, which consists of preparing solutions containing the sampled soil (TFSA – Fine Air-Dried Soil), sodium hexametaphosphate, and distilled water. The solutions were properly stirred (50 rpm), sieved to separate the sand fraction, and deposited in a 100 mL graduated cylinder for the identification of silt and clay.

Subsequently, the samples were agitated again and allowed to sediment following Stokes' Law. After mixing, 50 mL of the suspended material (collected at a depth of 5 cm from the graduated cylinder) was extracted using a volumetric pipette, deposited in beakers, and stored in an oven until complete evaporation for subsequent weighing of the fractions. Based on the results obtained from weighing and quantifying the sediments, the textural classification was performed according to the model proposed by Lemos and Santos (1996), which determines the soil class based on the percentage of clay, silt, and sand present in each sample.

In the chemical analyses, the results for pH, macronutrients, CEC, EC, and OM were assessed. The pH measurement was performed directly using the device, with TFSA homogenized in distilled water. Macronutrient analysis was conducted by separating 10 cm^3 of TFSA into a 125 mL Erlenmeyer flask, adding 100 mL of the required solution, agitating for 5 minutes at 180 rpm, and subsequently allowing it to decant for 24 hours. The results for Ca^{2+} and Mg^{2+} were obtained through titration using a 0.0125M EDTA (disodium salt) solution. Phosphorus (P) was identified using a photocolorimeter by observing the optical density of the solution extract. Potassium (K^+) and sodium (Na^+) were quantified using a flame photometer, based on readings from the device scale.

The analysis of organic matter (OM) involved weighing, sieving, grinding, and heating the TFSA. Afterward, the determination was conducted using the Walkley-Black method, which quantifies the organic carbon content in the soil through oxidation with potassium dichromate added to the sample, followed by titration with 0.05M ammonium ferrous sulfate (color change from blue to green). The cation exchange capacity (CEC) values were determined by summing the concentrations of Ca^{2+}, Mg^{2+}, K^{+}, and Al^{3+}. Electrical conductivity (EC) was assessed to estimate soil salinity by measuring cations and anions in the aqueous extract of soluble salts.

3. Results and Discussion

In presenting the results by individual points and parameters described in Table 2, the samples did not show results for Al^{3+}, m, and H+Al, except for P-237, which presented a value of 1.32 for the H+Al parameter. Regarding pH values, they were predominantly characterized as moderately alkaline (>7.4 to 8.3) (EMBRAPA, 2017), with the exception of P-240 (7.30) located in the Apflg and P-237 (6.90) from the Apfm, which were classified as neutral.

EC and ESP, in turn, are key parameters for identifying soil classification and its level of salinity. Thus, upon observing the relationship between these parameters, it is evident that the samples from Apf and Apfm follow a trend where ESP is higher than EC. Nevertheless, the Apflg showed a predominance of EC at points P-239 (ESP: 17; EC: 49.9) with low Na^{+} content, and P-241 (ESP: 80; EC: 104).

However, Apflg exhibited the highest EC values, influenced by the elevated Na^{+} content. Despite being under the influence of the main river channel and the effluent, the occasional freshwater influx does not impact the reduction of salinity, as flooding may dilute and transport salts from other regions (BORNMAN; ADAMS, 2010; RIDD; STIEGLITZ, 2002). Costa et al. (2014b), in characterizing the geochemistry along the Apodi-Mossoró River estuary, observed higher EC values (Average: 111.16 dS/m) near the main course, with the upper estuarine course being the area with the highest concentration, largely due to marine influence (ALBUQUERQUE et al., 2014a).

On the other hand, the sample closest to the main river channel in Apfm showed the highest organic matter (OM) concentration (P-319: 42.19 g/kg), possibly due to the biomass of the mangroves. The lowest concentration was identified in Apf, at P-234 (4.10 g/kg), a saline field with an elevation of 3m.

Table 2 – Values of soil analysis parameters for the upper estuarine course of the Apodi-Mossoró River. pH (soil:water 1:25); EC = Electrical Conductivity (soil:water extract); OM = Organic Matter; P = Phosphorus; K^{+} = Potassium; Na^{+} = Sodium; Ca^{2+} = Calcium; Mg^{2+} = Magnesium; Al^{3+} = Exchangeable Aluminum; H+Al = Potential Acidity; SB = Sum of Bases; t = Effective CEC; CEC = Cation Exchange Capacity; V = Base Saturation; m = Exchangeable Aluminum Saturation; ESP = Exchangeable Sodium Percentage.

Sample	pH	EC	OM	P	K^{+}	Na^{+}	Ca^{2+}	Mg^{2+}	Al^{3+}	H+Al	SB	t	CEC	V	m	ESP
	Water	dS/m	g/kg	cmolc/dm^3										%		
Fluvial plain (Apf); n = 5																
P-234 (05-15 cm)	7,50	18,20	4,10	0,32	1,38	73,48	15,60	9,90	0,0	0,0	100,39	100,39	100,40	100	0	73
P-235 (20-30 cm)	7,70	12,00	6,14	0,25	1,23	70,39	16,50	7,40	0,0	0,0	95,54	95,54	95,54	100	0	74
P-236 (10-20 cm)	7,80	11,60	4,51	0,32	1,20	46,50	12,50	8,60	0,0	0,0	68,83	68,83	68,83	100	0	68
P-237 (10-20 cm)	8,00	11,40	5,33	0,18	2,17	59,33	14,20	16,20	0,0	0,0	91,92	91,92	91,92	100	0	65
P-238 (20-30 cm)	8,10	12,50	7,78	0,21	2,24	54,47	17,70	14,10	0,0	0,0	88,53	88,53	88,53	100	0	62
Fluvio-lagoonal plain (Apfl); n = 3																
P-239 (05-15 cm)	7,60	49,9	4,51	0,23	3,74	13,33	7,20	53,4	0,0	0,0	77,69	77,69	77,69	100	0	17
P-240 (05-15 cm)	7,30	45,7	14,46	0,30	8,74	234,90	10,20	42,2	0,0	0,0	296,27	296,27	296,3	100	0	79

P-241 (05-15 cm)	7,40	104	15,26	0,20	7,21	239,44	8,40	44,8	0,0	0,0	299,95	299,95	300,0	100	0	80
Fluvio-marine plain (Apfm); n = 4																
P-317 (0-15cm)	6,90	14,06	7,30	0,42	0,85	28,56	11,10	11,64	0,0	1,32	52,16	52,16	53,48	98	0	53
P-318 (0-15cm)	8,10	3,76	17,04	0,58	1,56	10,08	4,70	6,94	0,0	0,0	23,29	23,29	23,29	100	0	43
P-319 (0-15cm)	7,80	24,00	42,19	0,10	3,92	80,48	8,10	14,73	0,0	0,0	107,27	107,27	107,27	100	0	75
P-320 (0-15cm)	8,00	12,00	5,68	0,33	0,98	29,88	22,60	15,24	0,0	0,0	68,71	68,71	98,71	100	0	44

Source: Authors (2022).

Among the sample groups, the highest and lowest concentrations of P were found in the Apfm samples, between P-318 (0.58) and P-319 (0.10), respectively, both located in mangrove forests, with P-318 being near a shrimp farming activity and P-319 near a salt production activity (Table 1). The presence of K^+ was more pronounced in the Apflg between points P-240 and P-241, with values of 8.74 cmolc/dm3 and 7.21 cmolc/dm3, respectively.

The descriptive statistics of the results presented in Table 3 for Apf, Apflg, and Apfm reveal significant variations among the results, with Na^+ and CEC parameters exhibiting the highest variances across all sample groups. In this regard, the Apf samples showed the lowest variances for CEC (177.97) and Na^+ (99.88), in contrast to the values from Apflg, where Na^+ (11137.00) and CEC (10798.92) displayed the highest variances among the samples. The Apfm, in turn, showed intermediate variances compared to the other environments. The micronutrient characterized by the least variation was P, a common scenario across all sample groups.

Table 3 – Descriptive statistics of soil analysis results from the upper estuarine course of the Apodi-Mossoró River. pH (soil:water 1:25); EC = Electrical Conductivity (soil:water extract); OM = Organic Matter; P = Phosphorus; K^+ = Potassium; Na^+ = Sodium; Ca^{2+} = Calcium; Mg^{2+} = Magnesium; Al^{3+} = Exchangeable Aluminum; H+Al = Potential Acidity; SB = Sum of Bases; t = Effective CEC; CEC = Cation Exchange Capacity; V = Base Saturation; m = Exchangeable Aluminum Saturation; ESP = Exchangeable Sodium Percentage.

	Minimum Value	**Maximum Value**	**Mean**	**Standard Deviation**	**Variance**	**Coefficient of Variation**
Samples from the fluvial plain (Apf); n = 5						
pH	7,50	8,10	7,82	0,21	0,05	0,03
EC	11,40	18,20	13,14	2,56	6,54	0,19
OM	4,10	7,78	5,57	1,31	1,71	0,23
P	0,18	0,32	0,26	0,06	0,00	0,23
K^+	1,20	2,24	1,64	0,46	0,21	0,28
Na^+	46,50	73,48	60,83	9,99	99,88	0,16
Ca^{2+}	12,50	17,70	15,30	1,81	3,27	0,12
Mg^{2+}	7,40	16,20	11,24	3,36	11,26	0,30
Al^{3+}	0,00	0,00	0,00	0,00	0,00	0,00
H+Al	0,00	0,00	0,00	0,00	0,00	0,00
SB	68,83	100,40	89,04	10,85	177,66	0,12
t	68,83	100,40	89,04	10,85	177,66	0,12
CEC	68,83	100,40	89,04	10,85	177,66	0,12
V	100	100	100	0,00	0,00	0,00
m	0,00	0,00	0,00	0,00	0,00	0,00
ESP	62,00	74,00	68,40	4,59	21,04	0,07
Samples from the fluvial-lagoonal plain (Apflg); n = 3						
pH	7,30	7,60	7,43	0,12	0,02	0,02
EC	45,70	104,00	66,53	26,55	704,82	0,40

OM	4,51	15,26	11,41	4,89	23,91	0,43
P	0,20	0,30	0,24	0,04	0,00	0,17
K^+	3,74	8,74	6,57	2,09	4,37	0,32
Na^+	13,33	239,44	162,56	105,53	11137,00	0,65
Ca^{2+}	7,20	10,20	8,60	1,23	1,52	0,14
Mg^{2+}	42,20	53,40	46,80	4,79	22,91	0,10
Al^{3+}	0,00	0,00	0,00	0,00	0,00	0,00
H+Al	0,00	0,00	0,00	0,00	0,00	0,00
SB	77,69	299,95	224,64	103,92	10798,92	0,46
t	77,69	299,95	224,64	103,92	10798,92	0,46
CEC	77,69	300,00	224,66	103,92	10798,92	0,46
V	100,00	100,00	0,00	0,00	0,00	0,00
m	0,00	0,00	0,00	0,00	0,00	0,00
ESP	17,00	80,00	58,67	29,47	868,22	0,50
Samples from the fluvio-marine plain (Apfm); n = 4						
pH	6,90	8,10	7,70	0,47	0,23	0,06
EC	3,76	24,00	13,45	7,21	51,94	0,54
OM	5,68	42,19	18,05	14,60	213,08	0,81
P	0,10	0,58	0,36	0,17	0,03	0,49
K^+	0,85	3,92	1,83	1,24	1,53	0,68
Na^+	10,08	80,48	37,25	26,16	684,33	0,70
Ca^{2+}	4,70	22,60	11,63	6,73	45,28	0,58
Mg^{2+}	6,94	15,24	12,14	3,30	10,90	0,27
Al^{3+}	0,00	0,00	0,00	0,00	0,00	0,00
H+Al	0,00	1,32	0,33	0,57	0,33	1,73
SB	23,29	107,27	62,86	30,36	921,69	0,48
t	23,29	107,27	62,86	30,36	921,69	0,48
CEC	23,29	107,27	62,86	30,36	921,69	0,48
V	98,00	100,00	99,50	0,87	0,75	0,01
m	0,00	0,00	0,00	0,00	0,00	0,00
ESP	43,00	75,00	53,75	12,87	165,69	0,24

Source: Authors (2022).

Moreover, the standard deviation results demonstrate heterogeneity in the sampling points, with Na^+ and CEC exhibiting the highest degree of dispersion in the Apf and Apflg samples; on the other hand, the parameters P, pH, K^+, Ca^{2+}, and OM appear more homogeneous, generally with values below 5. In the Apfm samples, the most homogeneous condition is limited to P, pH, and K^+. Thus, when comparing all the data presented in Table 3, it can be inferred that CEC exhibited the greatest dispersion, while P showed the least dispersion. The zone that exhibited the highest variability was Apflg, influenced by the river drainage and tidal advance, for which the standard deviation ranged from 105.53 for Na^+ to 103.94 for CEC.

The analysis through the average established between the parameters shows alternations in the fractions of EC, with 13.14 dS/m in Apf, 66.53 dS/m in Apflg, and 13.45 dS/m in Apfm. Thus, the results were higher than those identified in hypersaline wetlands located in the Monegros Desert, Spain, which presented an average of 6.58 dS/m, with variations from 0.33 dS/m to 16.30 dS/m (HERRERO; WINDORF; CASTANEDA, 2015). It is noteworthy that Embrapa (2017) characterizes soils with saturation greater than 7 dS/m as "saline" and toxic to most crops.

Regarding OM (g/kg), Apf resulted in 5.57, Apflg in 11.41, and Apfm, in turn, exceeded the values of the other groups, with 18.05. Concerning P, the highest average was identified in Apfm, with 0.55 cmolc/dm3; as for potassium (K+), the environment with the highest abundance was Apflg, with 6.57 cmolc/dm3. The ESP values indicate a sodic classification (≥ 15) for all samples (Apf: 68.40 / Apflg: 58.67 / Apfm: 53.75).

In the comparative analysis between the cations Na^+, Mg^{2+}, and Ca^{2+} (Figure 4), high concentrations of these ions are observed, with the highest levels found in Apflg, specifically in the samples P-240 and P-241. In general, the cation ratio revealed the following order: $Na^+ > Mg^{2+} > Ca^{2+}$, indicating Na^+ as the most abundant cation, a cationic pattern also observed in the evaporites of the plains of Canada (LAST, 1989). This high concentration occurs mainly in drainage-restricted environments with seawater impoundment and high evaporation rates, leading to the precipitation of soluble salts on the soil surface (SILVA; SCHREIBER; SANTOS, 2000; FANG; LIU; KEARNEY, 2005; ALBUQUERQUE et al.,

2014b; PEDROTTI et al., 2015; FREIRE et al., 2021). It can also occur through capillary rise of groundwater rich in salts, caused by the low pedological development with shallow depth and a predominance of primary minerals (ATTIA, 2013; JESUS; BORGES, 2020; FREIRE et al., 2021).

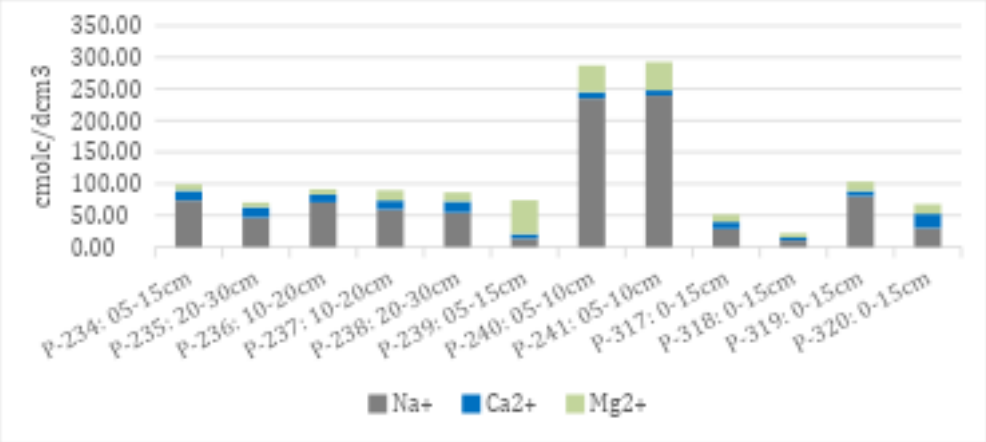

Figure 4 – Comparative analysis between the cations Na+, Ca2+, and Mg2+.
Source: Authors (2022).

The lowest concentration of Na^+ was found in the Apfm (P-318) with 10.08 cmolc/dm³, and P-239 is the only sample showing a higher concentration of Mg^{2+}. Ca^{2+}, in turn, had the highest concentration in sample P-320, with a total of 22.60 cmolc/dm³. Similarly, Costa et al. (2015) observed that the same hypersaline unit can exhibit variations in the nutrient accumulation pattern in sectors with distinct characteristics.

Thus, it is observed that the Apflg sector is the one with the greatest scarcity of vegetation cover (Table 1), primarily due to the high concentration of salts that hinders plant development, even for the most tolerant species (UCHOA; HADLICH; CELINO, 2008); on the other hand, in the environments of the other points, halophytic vegetation is present, demonstrating specific zones according to salinity parameters, highlighting the idea that hypersalinity conditions exhibit an irregular vegetation pattern (ALBUQUERQUE et al., 2014b).

It is also worth noting that the Apodi-Mossoró plain, influenced by the hypersaline estuary, is among the environments with the highest salt concentrations in natural areas (Table 4). Additionally, the significant heterogeneity of its chemical characteristics over the years can be highlighted, primarily influenced by the solar evaporation of seawater, which favors the large-scale production of sodium chloride in a sustainable manner, as salt flats form naturally, regardless of anthropogenic actions (COSTA et al., 2013).

Table 4 – Relationship of saline environments with different levels of salinity in average values.

Location	Na^+	Ca^{2+}	Mg^{2+}	EC	Source
	cmolc/dm³			dS/m	
Gulf of Aqaba, Egypt	145,12	13,64	26,19	93,00	Attia (2013)
Monegros Desert, Spain	-	-	-	6,58	Herrero; Windorf; Castaneda (2015)
Great Plains, Canada	66,16	0,94	10,23	-	Last (1989)
Apodi-Mossoró Estuary, Brazil	81,35	21,98	31,52	111,16	Costa et al. (2014)
Apodi-Mossoró Estuary, Brazil	96,49	22,49	23,58	58,66	Costa (2018)
Apodi-Mossoró Estuary, Brazil	133,55	21,84	43,92	48,71	Medeiros (2020)
Present research	78,40	12,40	20,43	26,59	

Source: Authors (2022).

In the soil texture classification, the granulometry of the sediments was analyzed through the relationship between sand, silt, and clay (Figure 5). It was observed that silt is the predominant granulometric fraction in the samples. Sand, in turn, is the least abundant fraction, and its highest concentrations were identified in the Apfm; the highest percentage of

clay, however, was found in the Apflg. It can be noted that the granulometry of Apf and Apflg show homogeneity with few variations between the textural classes, being Silty Loam (P-235, P-240, and P-241) and Silt (P-234, 236, 237, 238, and 239). In contrast, Apfm presented four types of classes: P-317 Silty Clay Loam, P-318 Loam, P-319 Silty Loam, and P-320 Silt. Overall, the samples showed a low sand content and a higher percentage of fine grains, similar to the sediments of the Aral Sea basin in Uzbekistan, which also presented a thin layer of halite between the pores (MEES; SINGER, 2006).

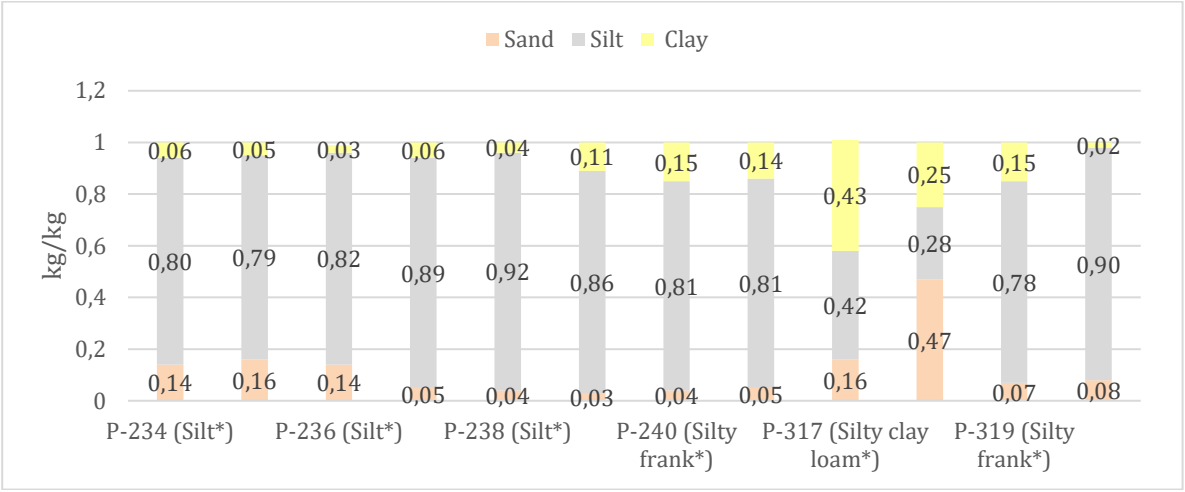

Figure 5 – Granulometric results of the sediments.
**Textural Classification.*
Source: Authors (2022).

4. Final Considerations

The soil under hypersaline influence showed heterogeneous characteristics across the analyzed parameters, even though the sampled points were within the same environment. However, throughout the entire upper estuarine area, high levels of salts were found, with Na^+ being the most abundant cation, followed by Mg^{2+} and Ca^{2+}, which directly influenced the fluctuations in CEC, ESP, and EC.

Furthermore, through the analysis of the ESP, EC, and pH parameters, it was found that the soil in all environments has a sodic classification, saline character, and moderately alkaline condition, reflecting the influence of the semiarid climate and the progressive evaporation of seawater in the supratidal area.

The high salinity levels negatively impact the vegetation cover, creating environments with extreme and toxic conditions for plants. The granulometry of the sediments, in turn, indicated a predominance of finer particles such as silt and clay, making the soil have a higher water retention capacity. This characteristic, combined with the constant flooding of the plain, contributes to the gleization process. Moreover, the Apfm zone was found to be the most diverse in terms of soil texture.

Acknowledgments

The present study was carried out with the support of the Coordination for the Improvement of Higher Education Personnel – Brazil (CAPES) – Funding Code 001, UFRN/PROPESQ (EDITAL N° 01/2024) financial support and the Soil, Water, and Plant Laboratory – LASAP (UFERSA) for their support in physical and chemical analyses.

References

ALBUQUERQUE, A. G. B. M. et al. Hypersaline tidal flats (apicum ecosystems): the weak link in the tropical wetlands chain. *Environmental Reviews*, v. 22, n. 2, p. 99-109, 2014a.

ALBUQUERQUE, A. G. B. M. et al. Soil genesis on hypersaline tidal flats (apicum ecosystem) in a tropical semi-arid estuary (Ceará, Brazil). *Soil Research*, v. 52, n. 2, p. 140-154, 2014b.

ATTIA, O. E. A. Sedimentological characteristics and geochemical evolution of Nabq sabkha, Gulf of Aqaba, Sinai, Egypt. *Arabian Journal of Geosciences*, v. 6, n. 6, p. 2045-2059, 2013.

BORNMAN, T. G.; ADAMS, J. B. Response of a hypersaline salt marsh to a large flood and rainfall event along the west coast of southern Africa. *Estuarine, Coastal and Shelf Science*, v. 87, n. 3, p. 378-386, 2010.

BRASIL. Lei nº 12.651, de 25 de maio de 2012. Institui o novo código florestal brasileiro.

BROWN, D. R. et al. Hypersaline tidal flats as important "blue carbon" systems: a case study from three ecosystems. *Biogeosciences*, v. 18, n. 8, p. 2527-2538, 2021.

COSTA, D. F. S et al. Caracterização geoquímica dos sedimentos em um ambiente hipersalino artificial. *Revista de Geociências do Nordeste*, v. 1, n. 1, p. 76-87, 2015.

COSTA, D. F. S. et al. Breve revisão sobre a evolução histórica da atividade salineira no estado do Rio Grande do Norte (Brasil). *Sociedade & Natureza*, v. 25, n. 1, p. 21–34, 2013.

COSTA, D. F. S. et al. Influência de macroaspectos ambientais na produção de sal marinho no litoral semiárido do Brasil. *Revista de Geografia (Recife)*, v. 31, n. 3, p. 28–42, 2014a.

COSTA, D. F. S. et al. Multifactorial analysis of the geochemical characterization in a Brazilian hypersaline floodplain. *Brazilian Journal of Aquatic Science Technology*, v. 18, p. 81-90, 2014b

COSTA, D. F. S.; ROCHA, R. M.; CESTARO, L. A. Análise fitoecológica e zonação de manguezal em estuário hipersalino. *Mercator*, v. 13, p. 119–126, 2014.

COSTA, D. F. S; SOUZA, Y. G; SOUZA, A. C. D. Fitogeografia e serviços ambientais prestados pelo manguezal do estuário do rio Apodi-Mossoró (RN). In: SOUZA, R. M; CHAVES, A. M. S; NASCIMENTO, S. P. G. (Eds.). *Geoecologia e Paisagem*. Aracajú, SE: Editora Criação, 2021.

COSTA, D. F. S; MOREIRA DA SILVA, D.E.; MEDEIROS, D. H. M.; FERNANDES, R. T. V.; DE MEDEIROS ROCHA, R. Aspectos naturais da zona estuarina do Rio Apodi-Mossoró (RN). In: CARVALHO, R. G. (Org.). *Rio Apodi-Mossoró:* meio ambiente e planejamento. Mossoró/RN: Edições UERN, 2022, p. 116 – 132.

COSTA, L. R. Atributos químicos e físicos do solo da planície hipersalina do estuário do Rio Apodi – Mossoró. 2018. 196 fl. (Tese de Doutorado). Programa de Pós-Graduação em Manejo de Solo e Água, Universidade Federal Rural do Semi-Árido (UFERSA). Mossoró/RN, 2018.

EMBRAPA. *Manual de Métodos de Análise de Solo*. 3. ed. Brasília, DF: EMBRAPA, 2017.

FANG, H.; LIU, G.; KEARNEY, M. Georelational analysis of doil type, soil salt content, landform, and land use in the Yellow River Delta, China. *Environmental Management*, v. 35, p. 72–83, 2005.

FREIRE, M. B. G. S. et al. Salinidade de solos: Problemas e soluções. In: FERNANDES, J. G.; CARVALHO, E. X. (Eds.) *Solos*: Estudos potencialidades e uso. Recife, PE: Instituto Agronômico de Pernambuco – IPA, 2021.

GANJU, N. K. et al. Spatially integrative metrics reveal hidden vulnerability of microtidal salt marshes. *Nature Communications*, v. 8, n. 1, p. 1-7, 2017.

GORDON, C. Hypersaline lagoons as conservation habitats: macro-invertebrates at Muni Lagoon, Ghana. *Biodiversity & Conservation*, v. 9, n. 4, p. 465-478, 2000.

GRIGORE, M. N.; TOMA, C. Saline environments. *Anatomical Adaptations of Halophytes*. *Springer International Publishing*, p. 29-37, 2017.

GUEDES, D. R. C.; SANTOS, N. M.; CESTARO, L. A. Planície flúvio-marinha do Rio Grande do Norte: uma abordagem geossistêmica. *Revista de Geociências do Nordeste*, v. 2, Número Especial, p. 821–831, 2016.

HERRERO, J.; WEINDORF, D. C.; CASTANEDA, C. Two fixed ratio dilutions for soil salinity monitoring in hypersaline wetlands. *PloS one*, v. 10, n. 5, 2015.

IBGE. Manual técnico da vegetação brasileira. Rio de Janeiro: *IBGE* (Manuais técnicos de geociências, n. 1) ed. 2. 2012.

JESUS, J; BORGES, M. T. Salinização de solos em Portugal. *Revista de Ciência Elementar*, v. 8, n. 3, p. 1-5, 2020.

KJERFVE, B. et al. Hydrology and salt balance in a large, hypersaline coastal lagoon: Lagoa de Araruama, Brazil. *Estuarine, Coastal and Shelf science*, v. 42, n. 6, p. 701-725, 1996.

LAST, W. M. Continental brines and evaporites of the northern Great Plains of Canada. *Sedimentary Geology*, v. 64, n. 4, p. 207-221, 1989.

LEMOS, R. C.; SANTOS, R. D. *Manual de descrição e coleta de solo no campo*. 3 ed. Campinas: Sociedade Brasileira de Ciência do Solo, 1996.

MEDEIROS, D. H. M. Influência da salinidade na heterogeneidade de paisagens estuarinas do domínio morfoclimático do semiárido brasileiro. 2020. 237 fl. Tese (Doutorado em Ciências Marinhas Tropicais) - Programa de Pós-Graduação em Ciências Marinhas Tropicais, Instituto de Ciências do Mar - LABOMAR, Universidade Federal do Ceará, Fortaleza, 2020.

MEES, F; SINGER, A. Surface crusts on soils/sediments of the southern Aral Sea basin, Uzbekistan. *Geoderma*, v. 136, n. 1-2, p. 152-159, 2006.

MIRANDA, L. B.; CASTRO, B. M.; KJERFVE, B. *Princípios de oceanografia física de estuários*. 2. ed. São Paulo: Editora da Universidade de São Paulo, 2002, 424 p.

OREN, A. Saltern evaporation ponds as model systems for the study of primary production processes under hypersaline conditions. *Aquatic Microbial Ecology*, v. 56, n. 2-3, p. 193-204, 2009.

PANKOVA, E. I. Salt-affected soils of the Eurasian Region: diagnostics, criteria and distribution. In: (Orgs) VARGAS, R. et al. *Handbook for saline soil management*. Roma: FAO/LMSU, 2018.

PEDROTTI, A. et al. Causas e consequências do processo de salinização dos solos. *Revista Eletrônica em Gestão, Educação e Tecnologia Ambiental*, v. 19, n. 2, p. 1308-1324, 2015.

PINHEIRO, L. S.; MORAIS, J. O. Interferências de barramentos no regime hidrológico do Estuário do Rio Catú-Ceará-Nordeste do Brasil. *Sociedade & Natureza*, v. 22, n. 2, p. 237-250, 2010.

RIDD, P. V.; STIEGLITZ, T. Dry season salinity changes in arid estuaries fringed by mangroves and saltflats. *Estuarine, Coastal and Shelf Science*, v. 54, n. 6, p. 1039-1049, 2002.

ROCHA, A. P. B. *Expansão urbana de Mossoró/RN (período de 1980 a 2004*): geografia, dinâmica e reestruturação do território. Mossoró/RN: Coleção O Mossoroense, 2005.

SHEN, C. et al. Salt dynamics in coastal marshes: Formation of hypersaline zones. *Water Resources Research*, v. 54, n. 5, p. 3259-3276, 2018.

SILVA, D. E. M; COSTA, D. F S. Classificação das áreas úmidas e seus macrohabitats na planície flúvio-marinha do rio Apodi-Mossoró/RN (litoral semiárido do Brasil). *Revista Brasileira de Geografia Física*, v. 15, n. 01, p. 602-617, 2022.

SILVA, M. A. M.; SCHREIBER, B. C.; SANTOS, C. L. Evaporites as mineral resources. *Revista Brasileira de Geofísica*, v. 18, p. 338-350, 2000.

SUGUIO, K. *Geologia Sedimentar*. São Paulo: Editora Blucher. 2003.

TUNDISI, J. G.; TUNDISI, T. M. *Limnologia*. São Paulo: Oficina de Textos, 2008.

UCHOA, J. M.; HADLICH, G. M.; CELINO, J. J. Apicum: transição entre solos de encostas e de manguezais. *Revista Educação, Tecnologia e Cultura*, p.58-63, 2008.